Design of a Low Mutual Coupling Antenna in a Circular Array Using EBG for Breast Tumor Detection

Muntaqo Alfin Amanaf
Department of Electrical Engineering, Institut Teknologi Sepuluh Nopember, Surabaya, Indonesia | Telecommunication Engineering Study Program, Telkom University, Purwokerto, Indonesia
7022221011@student.its.ac.id

Eko Setijadi
Department of Electrical Engineering, Institut Teknologi Sepuluh Nopember, Surabaya, Indonesia
ekoset@ee.its.ac.id (corresponding author)

Achmad Mauludiyanto
Department of Electrical Engineering, Institut Teknologi Sepuluh Nopember, Surabaya, Indonesia
maulud@ee.its.ac.id

Fannush Shofi Akbar
The University Center of Excellence for Intelligent Sensing-IoT, Telkom University, Surabaya, Indonesia
fannushakbar@telkomuniversity.ac.id

Received: 25 July 2025 | Revised: 21 September 2025 | Accepted: 5 October 2025

Licensed under a CC-BY 4.0 license | Copyright (c) by the authors | *DOI: https://doi.org/10.48084/etasr.13621*

ABSTRACT

Microwave imaging, used for breast tumor detection, requires low mutual coupling antennas in a circular array configuration, which can lead to signal degradation and distortion in the resulting images. This study proposes a Printed Monopole Antenna design with a Z-shaped slot Electromagnetic Band Gap (PMA-ZEBG) to minimize mutual coupling in a circular array configuration, resulting in a 13 dB decrease. The PMA-ZEBG is compact, measuring 35 × 40 × 1.524 mm ($0.30\lambda_0 \times 0.34\lambda_0 \times 0.01\lambda_0$ at 2.61 GHz), and has a bandwidth of 3.2 GHz (2.61 GHz–5.81 GHz). Simulated Specific Absorption Rate (SAR) values at 20 mm between the breast and the antenna indicate that the antenna is within safe standards for microwave imaging. The S-parameters from the PMA-ZEBG can be used to identify and localize tumor presence by employing the Delay and Sum (DAS) algorithm within the Microwave Radar-based Imaging Toolbox (MERIT). The imaging results obtained using the PMA-ZEBG antenna display a more defined tumor image within the specified area and fewer discernible spots on the periphery.

Keywords-breast tumor detection; circular array; electromagnetic band gap; mutual coupling

I. INTRODUCTION

X-ray mammography contributes to identifying breast tumors and has significantly reduced mortality by enabling early detection. However, this method has limitations, including high radiation exposure, high rates of false positives and false negatives, and unsuitability for women with dense breast tissue [1-3]. These limitations have led to the exploration of alternative diagnostic approaches, such as microwave imaging, an innovative technique for identifying and diagnosing breast conditions, including tumors. This method uses microwave signals to scan breast tissue and detect abnormalities by identifying differences in tissue composition [4]. Unlike traditional X-ray mammography, microwave imaging is non-ionizing, making it safer for repeated use because it eliminates the risk of radiation exposure. The proposed method uses the different dielectric properties of healthy and damaged tissue to distinguish between them, enabling earlier detection with greater sensitivity and less invasiveness than conventional methods. This technology relies on antennas to transmit and receive microwave signals, which are then processed to create detailed images of the breast. In a microwave breast imaging system, an antenna application uses several arrays with mutual coupling. When antenna elements in an array interact, distortions and inaccuracies in the measurements are produced, resulting in incorrect tissue

property estimations and poor-quality images [3, 5, 6]. Many techniques have been proposed to reduce mutual coupling in microwave imaging systems, such as parasitic [7], defected ground structure [8], and Electromagnetic Band Gap (EBG) [9], which includes effective surface wave suppression, preserved antenna performance, a compact design, and increased protection in dense arrays [10-12]. Authors in [13] proposed a Variable-Band-Stacked EBG (VBS-EBG) in order to reduce mutual coupling in E-shaped antennas for 5G applications by 16.16 dB and 6.05 dB at the first and second resonances of the Multiple-Input Multiple-Output (MIMO) antennas, respectively. The primary contribution of this research is the reduction of mutual coupling in circular arrays for breast tumor detection using an EBG. The majority of existing research has focused on linear or planar array configurations, leaving a notable gap in understanding and resolving this issue in circular arrays. Authors in [14] used Vivaldi antennas and metamaterial techniques to increase gain. However, high mutual coupling still occurs, with S_{21} and S_{91} values above -20 dB. This study proposes a PMA-ZEBG to minimize mutual coupling in circular arrays. Additional contributions involve integrating PMA antennas with EBG structures to detect breast tumors through microwave imaging, demonstrating a significant advancement in the field. Furthermore, simulation analysis of specific absorption rates in relation to the antenna's distance from breast tissue provides valuable insights into this technology's safety.

II. METHODOLOGY

The PMA-ZEBG was manufactured using Roger RO4003C material, which had a substrate thickness (h_s) of 1.524 mm, as well as a copper patch, ground plane, and feed with a thickness (h_p) of 0.035 mm. The RO4003C substrate has a dielectric constant of 3.55 and a loss tangent of 0.0027. The antenna's physical dimensions are 35 × 40 × 1.524 mm, corresponding to $0.30\lambda_o \times 0.34\lambda_o \times 0.01\lambda_o$ at the operating frequency of 2.61 GHz, as shown in Figure 1 and Table I. The PMA geometry began with a rectangular patch, which was adapted by cutting a quarter arc at the upper edge of the patch and decreasing the ground plane to increase the bandwidth [15]. Finally, a Z-shaped EBG slot was added to the left side of the PMA to reduce mutual coupling. The microwave breast imaging system for tumor detection is portrayed in Figure 2 (a), where the PMA-ZEBG was arranged in a 1×8 circular array to match the antenna position. Figure 2 (b) demonstrates that the circular array has an antenna element spacing (d_a) of 24.3 mm and a gap of 20 mm between the antenna and the breast surface (d_{ab}). The breast phantom diameter (D_{bp}) is set to 120 mm to simulate actual breast dimensions. The breast's diameter limits the circular array configuration to eight antennas. The parameters of the breast phantom model were specified by the permittivity, conductivity, density, and thickness of each tissue layer, as illustrated in Table II. The tissue layers contain skin, fat, glands, and tumors and are simulated using the CST Simulation Software. In the breast model simulation, a 20 mm tumor was placed at the coordinate (0, 0, 10). Figure 3 displays the experimental validation of the PMA-ZEBG prototype using Vector Network Analysis (VNA) measurements conducted in an anechoic chamber to accurately analyze the S-parameter and the antenna's radiation pattern.

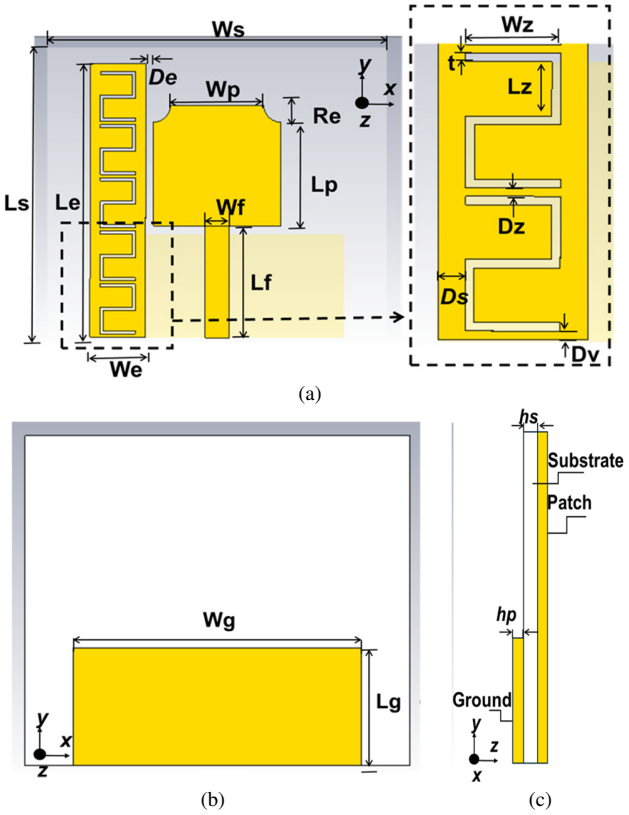

Fig. 1. Geometry design of the proposed antenna: (a) front view, (b) back view, (c) side view.

TABLE I. ANTENNA DIMENSIONS

Parameter	Value (mm)	Parameter	Value (mm)
Lg	12.5	*Ws*	40
Ls	35	*Wf*	2.85
Lf	13.5	*Wp*	11
Lp	12.5	*Re*	2
Wg	30	*Wz*	4.15
Le	33	*Lz*	2.44
We	6.55	*Dz*	0.38
De	0.25	*Dv*	0.37
Ds	1.2	*t*	0.38

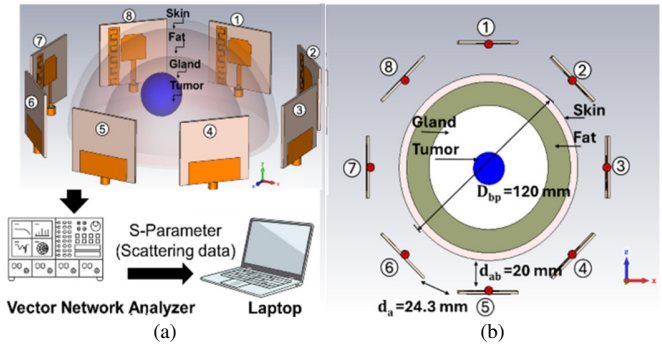

Fig. 2. (a) Microwave imaging system for tumor detection, (b) detail of circular array configuration.

TABLE II. BREAST TISSUE PROPERTIES IN THE BREAST PHANTOM MODEL [16, 17]

Tissue	Conductivity (S/m)	Permittivity (F/m)	Material density (kg/m^3)	Thickness (mm)
Skin	4	36	1100	5
Fat	0.4	9	700	15
Gland	0.45	13	1020	40
Tumor	4	50	1050	10

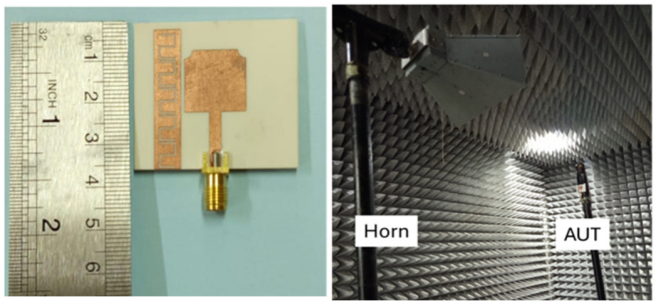

(a) (b)

Fig. 3. (a) Fabricated PMA-ZEBG antenna, (b) PMA-ZEBG measurement.

III. RESULTS AND DISCUSSION

Figure 4 presents a comparison of the S-parameter simulation graphs for PMA and PMA-ZEBG. The S_{11} parameter graph shows the resonance frequencies, frequency limits, and bandwidth.

The operating frequency can be determined from the S_{11} graph, which is below -10 dB. The graph shows that the antenna without the ZEBG has a frequency bandwidth of 3.58 GHz-6.00 GHz, whereas the PMA with ZEBG has a bandwidth of 2.61 GHz-5.74 GHz. The simulation results indicate that the PMA-ZEBG has a bandwidth of 3.13 GHz. There is a slight difference in the upper operating frequency limit between the simulation and measurement results: in the simulation, the operating frequency range is 2.61 GHz-5.74 GHz, whereas in the measurement, it is 2.61 GHz-5.81 GHz.

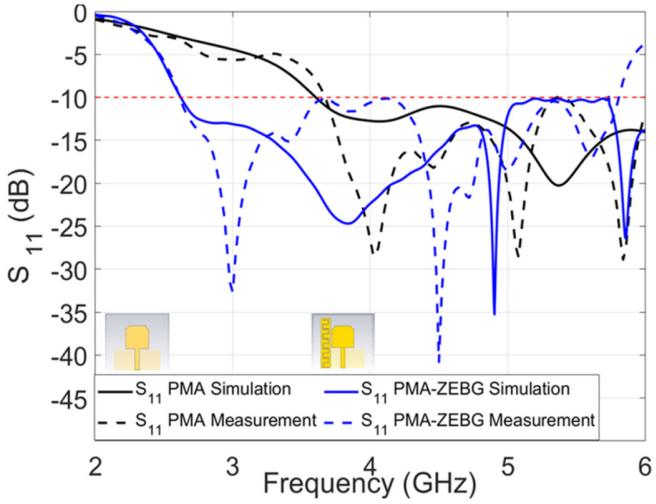

Fig. 4. Performance comparison between PMA and PMA-ZEBG through simulation and measurement analysis.

Figure 5 demonstrates that parameters S_{21} and S_{81} produce nearly identical graphs under both conditions. This phenomenon is also evident in the S_{31}-S_{71} and S_{41}-S_{61} parameter pairs, where identical graph patterns are observed. Mutual coupling can be detected by examining the graph below -20 dB on the S_{21} to S_{81} plot, in the 3.4 GHz – 4.5 GHz frequency range, with values above -20 dB reaching -18.2 dB, indicating a substantial degree of electromagnetic interaction between the antennas at these frequencies. Furthermore, examining the S_{21} and S_{81} PMA-ZEBG graphs within the same frequency range reveals a decrease in the S_{21} and S_{81} values, both of which decrease below -20 dB. Specifically, the S_{21} and S_{81} values decrease from -19 dB to -32 dB at 4.23 GHz, indicating a substantial reduction in mutual coupling at these frequencies. Adding the ZEBG significantly reduces the S_{21} and S_{81} parameters by 13 dB. This phenomenon can be attributed to the EBG system's ability to isolate mutual coupling from neighboring antennas, as portrayed in Figure 6. The neighboring antennas on the PMA-ZEBG have a smaller current distribution than the PMA. Consequently, ZEBG structures provide a high-impedance path for surface-wave propagation at specific operational frequencies, effectively mitigating mutual coupling.

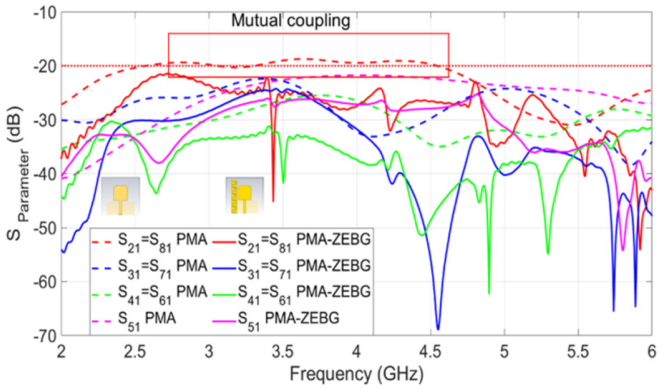

Fig. 5. A comparative analysis of the simulated S-parameter responses for PMA and PMA-ZEBG.

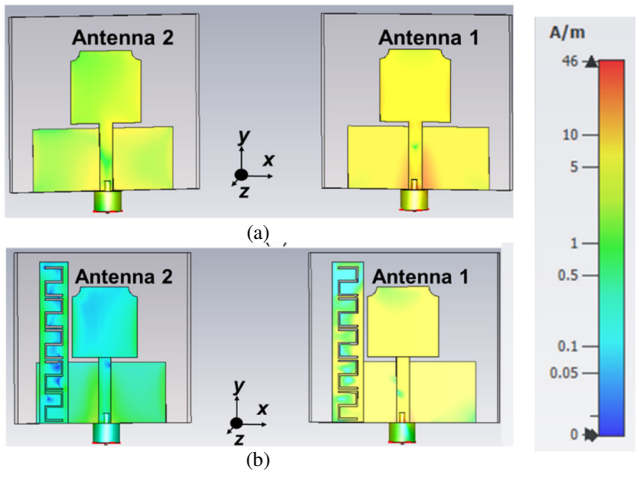

Fig. 6. Distribution of surface currents at 4 GHz (a) PMA, (b) PMA-ZEBG.

Figure 7 presents the simulations and measurements of the normalized radiation pattern in the E and H planes at frequencies of 3 GHz and 4 GHz, indicating that the antenna's main beam is directed towards the side of the antenna without the EBG, while moving away from the side with ZEBG. This is in accordance with the fundamental principle of the EBG operation, which involves suppressing surface waves and mutual coupling to direct the main beam.

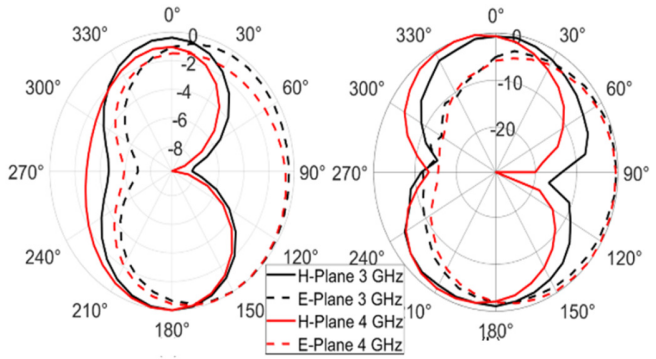

Fig. 7. Normalized radiation pattern: simulation (left), measurement (right).

The Envelope Correlation Coefficient (ECC) is a measure of the relationship between the signals received or transmitted by two antennas. A low ECC value means that the antennas operate independently with minimal mutual coupling. The ideal ECC value is close to 0, with the highest acceptable limit being 0.5 [18, 19]. Figure 8 depicts the ECC values from the PMA-ZEBG antenna simulation and measurement. The simulation shows a maximum value of 0.002 at a frequency of 2 GHz, while the measurement exhibits a maximum value of 0.006 at a frequency of 2.16 GHz. These results suggest that a low ECC value could support a microwave breast imaging system:

$$ECC = \frac{|S_{11}^{*}S_{12}+S_{21}^{*}S_{22}|^2}{(1-|S_{11}|^2-|S_{21}|^2)(1-|S_{22}|^2-|S_{12}|^2)} \quad (1)$$

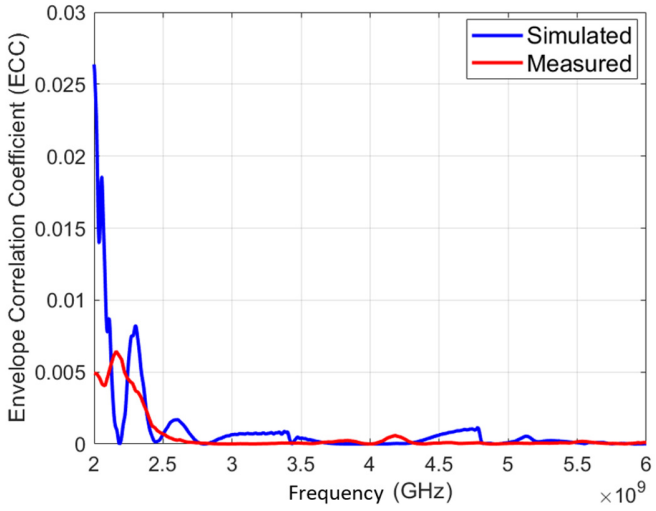

Fig. 8. The ECC of PMA-ZEBG circular array.

According to the mutual coupling analysis, this study significantly improves the isolation metric compared to previous studies on circular arrays for breast tumor detection. As displayed in Table III, this study achieves 32 dB of isolation, exceeding the values reported in previous studies of circular arrays.

TABLE III. PERFORMANCE COMPARISON BETWEEN THE PROPOSED AND THE PREVIOUS ANTENNA ARRAY

Ref.	Configuration	Technique	Dimension (λ_0)*	Frequency range (GHz)	Isolation $\|S_{21}\|$ (dB)
[8]	Linier	DGS	0.23×0.23 ×0.02	1.76-9.06	16
[14]	Circular	Metamaterial	0.30×0.26×0.01	2 – 10.45	18
[20]	Linier	EBG	1.35× 0.93×0.02	5.09 - 5.33	46
[21]	Linier	MM-EBG	0.50× 0.70×0.02	2.53 - 7.30	41
[22]	Circular	Partial Ground	0.52×0.52×0.02	3.4-7.4	18
[23]	Circular	CPW	0.39×0.39×0.01	3.9 – 19	16
This work	Circular	EBG	0.30×0.34×0.01	2.61 – 5.81	32

The safe level of pulse power, Specific Absorption Rate (SAR), signifies the rate at which energy is absorbed by or dissipated within tissue mass within a resonator volume:

$$SAR = \frac{\sigma|E|^2}{\rho} \quad (2)$$

where σ is the conductivity of the biological tissue, ρ is the mass density, and E is the induced electric field inside it. In this study, the SAR was determined by simulating the electric field within breast tissue using CST software. According to the IEEE C95.1 standard, an SAR value of 1 g of tissue should not exceed 1.6 W/kg, and an SAR value of 10 g of tissue should not exceed 2 W/kg [24, 25]. This study simulated an SAR with the distance between the antenna and breast ranging from 5 mm to 20 mm at 3 GHz, 4 GHz, and 5 GHz frequencies, respectively, in accordance with the antenna specifications. The purpose of this SAR simulation was to determine the safe distance between the breast and antenna to ensure that the SAR value did not exceed the safe limit. Figure 9 shows that increasing the distance between the antenna and breast correlates with a reduced maximum SAR value. This trend also occurs with higher frequencies. At a distance of 20 mm, the SAR value is below 1.6 W/kg for 1 g of cubic tissue at frequencies of 3GHz, 4GHz, and 5 GHz, and below 2 W/kg for 10 g of cubic tissue at these frequencies. The maximum SAR value at d_{ab} = 20 mm remains below the IEEE C95.1 standard's safe value [25]. Figure 10 illustrates the SAR distribution at d_{ab} = 20 mm with a frequency of 3 GHz in 1 g and 10 g of cubic tissue. The maximum SAR value in 1 g of cubic tissue was 1.15 W/kg at 3 GHz with a distance of 20 mm between the antenna and breast. In 10 g of tissue, the maximum SAR value is 1.79 W/kg at the same frequency and distance. The S-parameter simulation results for the PMA with and without the ZEBG were visualized using the DAS algorithm in the MERIT [14, 26]. The DAS algorithm delays the received signals to adjust for different travel times from a focal point inside the breast. Then, it sums the delayed signals coherently to enhance the location of the tumor while suppressing the noise and signals from other areas.

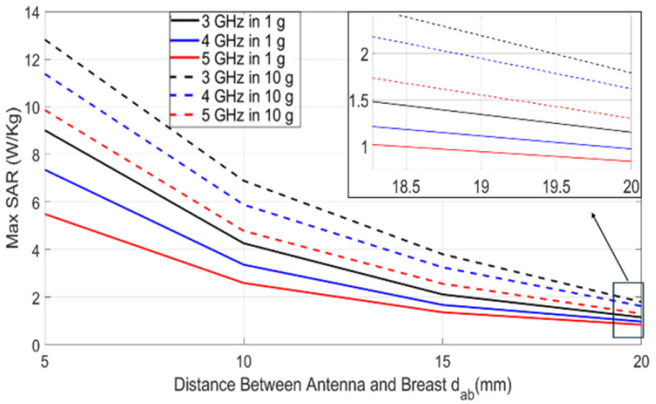

Fig. 9. Simulated maximum SAR in 1g and 10 g of cubic tissue.

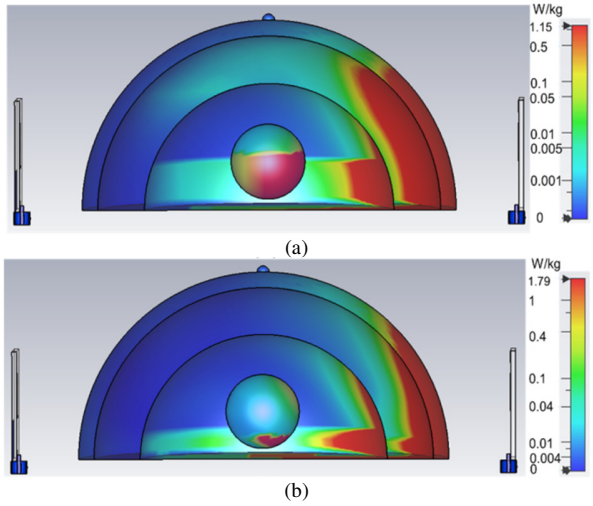

Fig. 10. SAR distribution at 3 GHz on d_{ab}= 20 mm in: (a) 1 g and (b) 10 g.

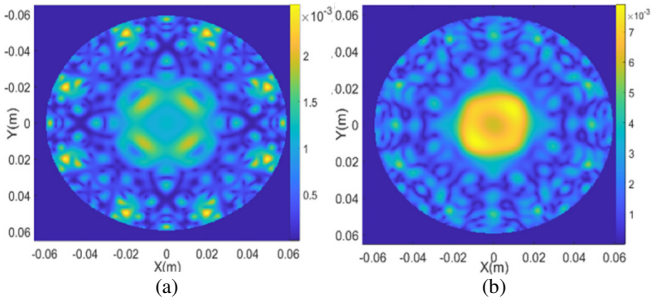

Fig. 11. Microwave imaging results for breast tumor detection: (a) without ZEBG, (b) with ZEBG.

Figure 11 shows the results of microwave imaging of a breast phantom with a tumor, using an antenna without ZEBG, revealing a faint tumor in both the central and peripheral regions of the breast. This indicates inaccuracies in tumor interpretation at these locations due to mutual coupling between the antennas. Concurrently, the imaging results obtained with the ZEBG antenna displayed a more defined yellow tumor within the tumor area and less discernible spots on the periphery. The PMA-ZEBG antenna can locate and pinpoint the position of a tumor within a microwave imaging system designed for breast tumor detection.

IV. CONCLUSIONS

This study designed, analyzed, and examined a printed monopole antenna with a Z-shaped slot Electromagnetic Band Gap (EBG) structure to minimize mutual coupling in a circular array configuration. The proposed antenna has a compact size of 35 mm × 40 mm × 1.524 mm, corresponding to 0.30λ0 × 0.34λ0 × 0.01λ0 at a frequency of 2.61 GHz. The PMA-ZEBG also exhibits a 3.2 GHz bandwidth, spanning from 2.61 GHz to 5.81 GHz. Incorporating the Z-shaped slot EBG into the printed monopole antenna significantly reduced mutual coupling by 13.11 dB, ranging from -19 dB to -32 dB at 4.23 GHz. Furthermore, the Envelope Correlation Coefficient (ECC) value was found to be below 0.5, indicating low mutual coupling. The simulated Specific Absorption Rate (SAR) value at a distance of 20 mm between the breast and antenna was within the safe standard for microwave imaging. Additionally, the S-parameter of the PMA-ZEBG antenna can be used with the Delay and Sum (DAS) algorithm in the Microwave Radar-Based Imaging Toolbox (MERIT) to detect and identify cancer locations. The imaging results using the PMA-ZEBG antenna showed a clearer tumor image within the tumor area and fewer discernible spots on the periphery.

ACKNOWLEDGMENT

This research was supported by the Indonesian Ministry of Higher Education, Science, and Technology, the Center for Higher Education Funding and Assessment (PPAPT), and the Indonesia Endowment Fund for Education (LPDP), through the Beasiswa Pendidikan Indonesia, grant number 202209092331.

REFERENCES

[1] M. A. Aldhaeebi, K. Alzoubi, T. S. Almoneef, S. M. Bamatraf, H. Attia, and O. M. Ramahi, "Review of Microwaves Techniques for Breast Cancer Detection," *Sensors*, vol. 20, no. 8, Jan. 2020, Art. no. 2390, https://doi.org/10.3390/s20082390.

[2] U. Rafique, S. Pisa, R. Cicchetti, O. Testa, and M. Cavagnaro, "Ultra-Wideband Antennas for Biomedical Imaging Applications: A Survey," *Sensors*, vol. 22, no. 9, Jan. 2022, Art. no. 3230, https://doi.org/10.3390/s22093230.

[3] T. Saeidi, S. N. Mahmood, S. Saleh, N. Timmons, A. J. A. Al-Gburi, and F. Razzaz, "Ultra-wideband (UWB) antennas for breast cancer detection with microwave imaging: A review," *Results in Engineering*, vol. 25, Mar. 2025, Art. no. 104167, https://doi.org/10.1016/j.rineng.2025.104167.

[4] H. M. E. Misilmani, T. Naous, S. K. A. Khatib, and K. Y. Kabalan, "A Survey on Antenna Designs for Breast Cancer Detection Using Microwave Imaging," *IEEE Access*, vol. 8, pp. 102570–102594, 2020, https://doi.org/10.1109/ACCESS.2020.2999053.

[5] S. N. Mahmood *et al.*, "A Bra Monitoring System Using a Miniaturized Wearable Ultra-Wideband MIMO Antenna for Breast Cancer Imaging," *Electronics*, vol. 10, no. 21, Jan. 2021, Art. no. 2563, https://doi.org/10.3390/electronics10212563.

[6] N. AlSawaftah, S. El-Abed, S. Dhou, and A. Zakaria, "Microwave Imaging for Early Breast Cancer Detection: Current State, Challenges, and Future Directions," *Journal of Imaging*, vol. 8, no. 5, May 2022, Art. no. 123, https://doi.org/10.3390/jimaging8050123.

[7] F. Amillia, E. Setijadi, and G. Hendrantoro, "The Effect of Parasitic Patches Addition on Bandwidth Enhancement and Mutual Coupling in 2 × 2 Sub-Arrays," *IEEE Access*, vol. 10, pp. 72057–72064, 2022, https://doi.org/10.1109/ACCESS.2022.3185999.

[8] P. S. Chowdary and S. K. Panda, "Performance Analysis of a Swastika shaped MIMO Antenna for Wireless Communication Applications," *Engineering, Technology & Applied Science Research*, vol. 15, no. 1, pp. 19971–19976, Feb. 2025, https://doi.org/10.48084/etasr.9478.

[9] I. Iliev, M. Nedelchev, and E. Markov, "A Novel 2D Z-Shaped Electromagnetic Bandgap Structure," *Engineering, Technology & Applied Science Research*, vol. 5, no. 1, pp. 760–763, Feb. 2015, https://doi.org/10.48084/etasr.530.

[10] S. E and P. G, "Enhancing MIMO Antenna Isolation with Novel Electromagnetic Band Gap (EBG) Structure and Genetic Algorithm Optimization," *Applied Artificial Intelligence*, vol. 38, no. 1, Dec. 2024, Art. no. 2344143, https://doi.org/10.1080/08839514.2024.2344143.

[11] A. Kumar, A. Q. Ansari, B. K. Kanaujia, J. Kishor, and L. Matekovits, "A review on different techniques of mutual coupling reduction between elements of any MIMO antenna. Part 2: Metamaterials and many more," *Radio Science*, vol. 56, no. 3, pp. 1–22, Mar. 2021, https://doi.org/10.1029/2020RS007222.

[12] M. Ebrahimpouri, E. Rajo-Iglesias, Z. Sipus, and O. Quevedo-Teruel, "Cost-Effective Gap Waveguide Technology Based on Glide-Symmetric Holey EBG Structures," *IEEE Transactions on Microwave Theory and Techniques*, vol. 66, no. 2, pp. 927–934, Oct. 2018, https://doi.org/10.1109/TMTT.2017.2764091.

[13] K. S. L. Parvathi and S. R. Gupta, "Novel dual-band EBG structure to reduce mutual coupling of air gap based MIMO antenna for 5G application," *AEU - International Journal of Electronics and Communications*, vol. 138, Aug. 2021, Art. no. 153902, https://doi.org/10.1016/j.aeue.2021.153902.

[14] M. T. Islam, M. T. Islam, M. Samsuzzaman, H. Arshad, and H. Rmili, "Metamaterial Loaded Nine High Gain Vivaldi Antennas Array for Microwave Breast Imaging Application," *IEEE Access*, vol. 8, pp. 227678–227689, 2020, https://doi.org/10.1109/ACCESS.2020.3045458.

[15] M. A. Amanaf, E. Setijadi, A. Mauludiyanto, and F. S. Akbar, "Bandwidth and Gain Enhancement of Rectangular Antenna with Upper Corner Etching and Partial Ground for Microwave Breast Imaging Applications," in *2023 6th International Seminar on Research of Information Technology and Intelligent Systems (ISRITI)*, Batam, Indonesia, Sept. 2023, pp. 197–201, https://doi.org/10.1109/ISRITI60336.2023.10467527.

[16] S. Subramanian, B. Sundarambal, and D. Nirmal, "Investigation on Simulation-Based Specific Absorption Rate in Ultra-Wideband Antenna for Breast Cancer Detection," *IEEE Sensors Journal*, vol. 18, no. 24, pp. 10002–10009, Sept. 2018, https://doi.org/10.1109/JSEN.2018.2875621.

[17] K. Brinda, S. Kumar P, N. Priyadharshini, S. K. C, D. S. Prasanth, and R. Agarwal, "Design of Ultra-Wideband Planar Monopole Antenna for Breast Tumor Detection," in *2019 International Conference on Vision Towards Emerging Trends in Communication and Networking (ViTECoN)*, Vellore, India, Mar. 2019, pp. 1–4, https://doi.org/10.1109/ViTECoN.2019.8899455.

[18] S. Mandal and C. K. Ghosh, "Low Mutual Coupling of Microstrip Antenna Array Integrated with Dollar Shaped Resonator," *Wireless Personal Communications*, vol. 119, no. 1, pp. 777–789, July 2021, https://doi.org/10.1007/s11277-021-08237-1.

[19] C. Hao, H. Zheng, Y. Gu, and X. Sun, "Mutual Coupling Reduction of MIMO Antenna Array Using Meta-FCRR," *Wireless Personal Communications*, vol. 119, no. 4, pp. 3435–3445, Aug. 2021, https://doi.org/10.1007/s11277-021-08415-1.

[20] A. Louaifi, Z. Laieb, and Y. Lamhene, "A novel hybrid design methodology for EBG structures with application to mutual coupling reduction in antenna arrays," *Journal of Computational Electronics*, vol. 24, no. 3, Apr. 2025, Art. no. 73, https://doi.org/10.1007/s10825-025-02312-7.

[21] P. Kumar, R. Sinha, A. Choubey, and S. K. Mahto, "A Novel Metamaterial Electromagnetic Band Gap (MM-EBG) Isolator to Reduce Mutual Coupling in Low-Profile MIMO Antenna," *Journal of Electronic Materials*, vol. 51, no. 2, pp. 626–634, Feb. 2022, https://doi.org/10.1007/s11664-021-09310-y.

[22] Y. Rahayu, R. Rosdiansyah, R. Amri, and R. Ngah, "A Novel Design Circular UWB Antenna Array for Microwave Breast Tumor Detection," in *2019 8th Asia-Pacific Conference on Antennas and Propagation (APCAP)*, Incheon, South Korea, Dec. 2019, pp. 75–76, https://doi.org/10.1109/APCAP47827.2019.9472165.

[23] H. Li, H. Zhang, Y. Kong, and C. Zhou, "Flexible Dual-Polarized UWB Antenna Sensors for Breast Tumor Detection," *IEEE Sensors Journal*, vol. 22, no. 13, pp. 13648–13658, July 2022, https://doi.org/10.1109/JSEN.2022.3180356.

[24] W. Bouamra, I. Sfar, A. Mersani, L. Osman, and J. M. Ribero, "A Low-Profile Wearable Textile Antenna Using AMC for WBAN Applications at 5.8GHz," *Engineering, Technology & Applied Science Research*, vol. 12, no. 4, pp. 9048–9055, Aug. 2022, https://doi.org/10.48084/etasr.5011.

[25] C95.1-2005 IEEE Standard for Safety Levels with Respect to Human Exposure to Radio Frequency Electromagnetic Fields, 3 kHz to 300 GHz. New York, NY, USA: IEEE, 2006.

[26] D. O'Loughlin *et al.*, "Open-source software for microwave radar-based image reconstruction," in *12th European Conference on Antennas and Propagation (EuCAP 2018)*, London, UK, Apr. 2018, pp. 1–4, https://doi.org/10.1049/cp.2018.0767.